

Study of Side-Chain Copolymers Containing H-Bonded / Covalent Bent-Core Mesogen

Graduate student: Hsin-Yi Tsai

Advisor: Dr. Hong-Cheu Lin

Department of Materials Science and Engineering

National Chiao Tung University

Abstract

Conventional free radical polymerization has been used to synthesize side-chain copolymers with H-bonded/covalent bent-core mesogen. The molar ratio of resulting polymers exhibiting smectic layer arrangement is characterized by NMR spectroscopy. The synthesis of the desired bent-core complexes required two components (H donor and H acceptor) to be mixed in precise equimolecular proportions in a common solvent (THF) followed by removal of the solvent. Differential scanning calorimetry, thermo-polarized optical microscopy, wide-angle X-ray diffraction are used to characterized the liquid crystal phases of all studied materials involving covalent low molecular weight bent-core mesogens, acrylate monomers and side-chain H-bonded complexes. The electro-optic measurement is carried out by applying a triangular wave field. It is not until the constitutional ratio of H-bonded/covalent bent-core mesogen in copolymer was tuned to 10/1 that the complex exhibit ferroelectric (FE) property. Only one current peak can be clearly identified within a modified triangular wave indicating the FE behavior and P_s value is measured to be 50~130 nCcm⁻².

含氫鍵與共價鍵彎曲型液晶基側鏈共聚高分子之研究

研究生：蔡馨儀

指導教授：林宏洲

國立交通大學材料科學與工程研究所

碩士班

摘要

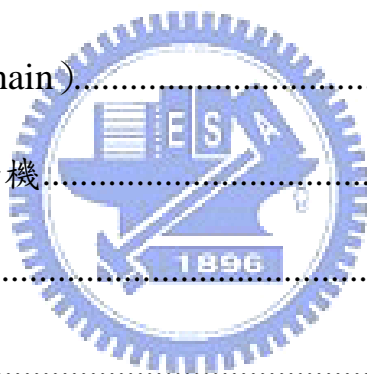
含氫鍵與共價鍵彎曲型共聚高分子運用常見自由基聚合已被成功合成出。此系列共聚高分子液晶相為層狀排列結構，可藉由核磁共振光譜儀估算氫鍵部份佔整體共聚高分子比例。將二種成份（分別為質子予體與質子受體）以當量比 1:1 含量共同溶四氫氟喃溶劑，待溶劑自然揮發即合成出所需彎曲型錯合物。藉由示差掃描熱量計、偏光顯微鏡及廣角 X 光繞射，鑑定本實驗開發材料，其中包括共價鍵小分子香蕉型液晶、壓克力基單體與側鏈型氫鍵錯合物。並且運用三角波電壓法量測所有材料光電特性。本實驗發現，當氫鍵與共價鍵組成比例為 10:1 時，其氫鍵錯合物展現鐵電行為，即使使用修飾三角波，在半週期處發現一根明顯特徵峰，為典型鐵電特性。其自發極化值大約 $50\sim 130 \text{ nCcm}^{-2}$ 。

目錄

摘要.....	I
目錄.....	II
圖目錄.....	III
表目錄.....	IV
附圖目錄.....	V
第一章緒論.....	1
1-1 前言.....	2
1-2 液晶簡介.....	3
1-2-1 何謂液晶.....	3
1-2-2 液晶分類.....	4
1-2-3 液晶性質.....	5
1-2-4 液晶觀察與識別.....	8
1-3 鐵電型液晶.....	9
1-3-1 何謂鐵電&鐵電型液晶.....	9
1-3-2 鐵電型液晶之化學結構.....	10
1-4 反鐵電型液晶.....	12
1-5 香蕉型液晶.....	14
1-5-1 非旋光性(achiral or nonchiral)分子旋光性質.....	16



1-5-2 極性切換(Polar switching)機制.....	17
1-5-3 小分子香蕉型液晶.....	21
1-5-4 寡分子香蕉型液晶.....	24
1-5-5 高分子香蕉型液晶.....	25
1-6 超分子(Supramolecular)氫鍵型液晶.....	26
1-6-1 氫鍵型液晶分子歷史.....	27
1-6-2 自我組裝氫鍵液晶分子分類.....	28
1-6-2-1 主鏈型(Main-chain).....	29
1-6-2-2 側鏈型(Side-chain).....	30
1-7 文獻回顧與研究動機.....	32
第二章實驗部份.....	33
2-1 實驗藥品.....	34
2-2 實驗儀器.....	36
2-3 合成流程.....	39
2-4 合成步驟.....	42
第三章結果與討論.....	62
3-1 合成機制探討.....	63
3-1-1 Williamson 醚化反應.....	63
3-1-2 脫水反應.....	63



3-1-3 Suzuki Coupling.....	64
3-2 共價鍵小分子香蕉型液晶.....	65
3-2-1 液晶熱性質結果.....	66
3-2-2 X光粉末繞射(Powder X-ray)研究.....	68
3-2-3 光電研究.....	70
3-2-3-1 液晶之填充.....	70
3-2-3-2 光電量測之裝置.....	71
3-2-3-3 液晶相分子層與層之間傾斜判定.....	74
3-3 氫鍵小分子香蕉型液晶.....	75
3-3-1 液晶熱性質結果.....	76
3-3-2 X光粉末繞射(Powder X-ray)研究.....	79
3-3-3 光電研究.....	80
3-3-3-1 自發極化值量測.....	80
3-3-3-2 液晶相分子層與層之間傾斜判定.....	82
3-4 壓克力基單體.....	83
3-4-1 單體熱性質結果.....	84
3-4-2 X光粉末繞射(Powder X-ray)研究.....	87
3-4-3 光電研究.....	88
3-5 側鏈型共聚高分子.....	90
3-5-1 高分子構型設計.....	90



3-5-2 結構命名&高分子基本性質.....	91
3-5-3 高分子氫鍵鑑定.....	94
3-5-3 高分子熱性質結果.....	95
3-5-5 X光粉末繞射(Powder X-ray)研究.....	99
3-5-6 光電研究.....	101
第四章結論.....	106
參考文獻.....	109



圖目錄

Fig. 1-3.1 The bistates of the ferroelectric liquid crystals.....	11
Fig. 1-3.2 The helical structure of SmC* phase. P: the polar direction, C: C-director, θ : tilted angle, ψ : azimuthal angle.....	12
Fig. 1-4.1 The structures of ferroelectric phase, ferroelectric phase and antiferroelectric phase.....	13
Fig. 1-4.2 The molecular arrangement of (a) helical state in antiferroelectric liquid crystal phase, (b) unwound state in antiferroelectric liquid crystal phase, (c) helical state in ferroelectric liquid crystal phase.....	14
Fig. 1-5.1 (a) Schematic representation of a typical achiral bent-core molecule (b) parallel and antiparallel packing of columns of bowl-shaped molecule.....	15
Fig. 1-5.2 Basic structural models proposed for some of the mesophases reported for bent-core liquid crystals.....	16
Fig. 1-5.3 Four types of the SmCP phase, which are distinguished by the relative tilt sense and the polar order (which corresponds to the bent direction) in adjacent smectic layers. The suffixes S or A, added to the C, define whether the tilt is synclinic or anticlinic. The suffixes F and A, after P, refer to ferroelectric or antiferroelectric polar orders. Full and open molecular symbols indicate smectic layers of opposite handedness (n: director, k: layer normal, p: polar axis). The signs \oplus and \odot correspond to opposite bent directions.....	17
Fig. 1-5.4 Mechanisms of polar switching (a) by collective rotation of the molecules around their long axes and (b) by rotation of the director	

around the tilt cone. Filled and open molecule symbols designate layers of opposite handedness.....18

Fig. 1-5.5 Rotation of the dark extinction brushes in circular domains as seen between crossed polarisers (position of polariser P and analyser A are indicated by arrows) for an AF mesophase with $SmC_A P_A$ ground state structure under a dc electric field on reversing the sign of the applied field, demonstrating the tristable switching. (a) Fieldinduced FE state ($SmC_S P_F$); (b) AF ground state ($SmC_A P_A$) and (c) FE state ($SmC_S P_F$) with opposite polar direction. A schematic representation of the arrangement of the molecules in the circular domains with equidistant smectic layers (cross-sectional area parallel to the cell surfaces) responsible for the occurrence of dark brushes and a simplified presentation of only a part of these domains are shown below.....19

Fig. 1-5.6 Optical photomicrographs showing the switching of the racemic $SmC_S P_A$ phase as seen between crossed polarisers and models showing the reorganisation of the molecules during the switching process around a cone. (a) Field-induced FE state ($SmC_A P_F$); (b) AF ground state ($SmC_S P_A$) composed of domains with opposite tilt direction and anticlinic/FE boundaries between them (areas with yellow background), and (c) FE state ($SmC_A P_F$) with opposite polarity.....20

Fig. 1-5.7 The general structure of bent-core molecules and positions of structural variations.....21

Fig. 1-5.8 The general structure of bent-core molecules with substituents on central bent unit.....23

Fig. 1-5.9 Influence of the position of F-substituents at the bent aromatic core upon the liquid crystalline properties of the resorcinol derived

phenylbenzoates (at least one position S1~S4 is substituted by F).....	24
Fig. 1-6.1 Schematic representation of four typical H-bonded liquid crystals.....	28
Fig. 1-6.2 The chemical structures of main-chain H-bonded polymers.....	30
Fig. 1-6.3 Carboxyl/pyridine system of side-chain H-bonded polymers.....	31
Fig. 1-6.4 Carboxyl/amino-pyridine system of side-chain H-bonded polymers.....	31
Fig. 3-1.1 Chemical Structures of three analogous of bent-core molecules under investigation.....	66
Fig. 3-2.1 Optical photomicrographs (crossed polarizers)of the B ₁ phase of BiphPEO as obtained by cooling from the isotropic liquid: (a) growth of dendritic nuclei at 134°C, (b) mosaic-like texture at 140 °C.....	68
Fig. 3-2.2 Optical photomicrographs (crossed polarizers) of the B ₂ phase of BiphN as obtained by cooling from the isotropic liquid: (a) Schlieren texture and fan-shaped texture at 140 °C, (b) spherulites domains at 148 °C.....	68
Figure 3-2.3 X-ray diffraction intensity against angle profiles obtained upon cooling from the isotropic phase: (a) in the B ₁ phase of compound BiphPEO at 110 °C; (b) in the B ₂ phase of compound BiphN at 140 °C.....	70
Figure 3-2.4. Schematic illustration of injection processes of liquid crystals materials by means of the vacuum oven.....	71

Fig. 3-2.5 The experimental installation for measurement of switching current response.....	72
Fig. 3-2.6 Switching current response in the SmCP _A phase of compound BiphN obtained by applying a triangular voltage ($V_{pp} = 102$ V, $f = 50$ Hz, $T = 140$ °C).....	73
Fig. 3-2.7 Ps value dependence on temperature variation for a fixed triangular wave field of $V_{pp} = 100$ V, $f = 50$ Hz.....	73
Fig. 3-2.8 Optical micrographs (crossed polarizers) taken from a racemic region of compound BiphN in the B ₂ phase by applying electric dc voltage (± 50 V).....	75
Figure 3-3.1. General structures of the three H-bonded complexes 12BAN , H12BAN , and AC12BAN containng H donors and acceptors.....	76
Fig. 3-3.2 Optical photomicrograph (crossed polarizers) obtained by cooling from the isotropic liquid: (a) spherulites domains of compound 12BAN , (b) highly ordered crystalline phase of compound H12BAN , (c) highly ordered crystalline phase of compound AC12BAN	78
Fig. 3-3.3 Transition temperatures of the three H-bonded bent-core molecules; blue parts of the columns represent one crystalline phase and purple parts represent other crystalline phase.....	79
Fig. 3-3.4 X-ray diffraction patterns for H-bonded molecules of (a) AC12BAN at 95 °C, (b) 12BAN at 104 °C.....	80
Fig 3-3.5 A profile showing the time dependence of the polarization current obtained for the SmCP _A phase of compound 12BAN at 104 °C under a triangular electric field ($V_{pp} = 180$ V, $f = 100$ Hz).....	81

Fig 3-3.6 Ps value dependence on: (a) frequency variation at $V_{pp} = 111$ V, $T = 103$ °C; (b) voltage variation at $f = 60$ Hz, $T = 106$ °C	81
Fig 3-3.7 Optical micrographs (crossed polarizers) taken from a chiral region of compound 12BAN in the B_2 phase by applying electric dc voltage (± 90 V).....	82
Fig. 3-4.1 Designed chemical structures of acrylate monomers.....	84
Fig. 3-4.2 Optical photomicrographs (crossed polarizers) of monomer MACBiph6 : (a) as obtained by fast cooling from isotropic liquid, (b) the magnification of (a), (c) exhibited unspecific texture by applying a shear force.....	86
Fig. 3-4.3 Optical photomicrographs (crossed polarizers): (a) schlieren texture of monomer ACBiph5 at 88 °C, (b) grain texture of monomer ACBiph5 by applying a shear force, (c) crystalline phase of monomer ACBenz5 at 70 °C	86
Fig. 3-4.4 Differential scanning calorimetry thermograms of MACBiph6 , ACBiph5 and ACBenz5 at heating and cooling rate of 10 °C mm^{-1}	86
Fig. 3-4.5 Wide-angle X-ray diffraction profile of MACBiph6 at 140 °C and ACBenz5 at 80 °C	88
Fig. 3-5.1 General structures of side-chain H-bonded copolymers and their monomers.....	92
Fig. 3-5.2 IR spectrum of the all complexes in which the molar ratio of hydroxyl to pyridine ring is 1:1 for: (a) low molecular weight of 12BAN , (b) homopolymer/copolymer of HA1B0N , CA10B1N , CA1B3.5N	95

Fig 3-5.3 Polarized light microscope image of Homopolymer HA1B0N : (a) for circular domain, (b) for schlieren texture.....	96
Fig. 3-5.4 Optical microscopic textures for the smetic phase of polymers: (a) CA10B1N (140 °C), (b) CA4B1N (140 °C), (c) CA1B3.5N (145 °C), (d) CA10C1N (124 °C), (e) HA0B1 (124 °C).	96
Fig. 3-5.5 DSC thermogram for copolymer CA10B1N. The heating and cooling rate was 10 °C min ⁻¹	97
Fig. 3-5.6 Transition temperatures of the all complexes and H-bonded low molecular weight compound AC12BAN ; blue parts of the columns represent one crystalline phase and purple parts represent other crystalline phase.....	99
Fig. 3-5.7 X-ray diffractogram obtained for: (a) compounds HA1B0 in the mesophase at 133 °C (black line) and (b) complex HA1B0N in the mesophase at 100 °C.	100
Fig. 3-5.8 Compare of X-ray diffraction pattern for homopolymers and copolymers.....	101
Fig. 3-5.9 Switching current response on applying a triangular wave voltage at a frequency of 150 Hz (T = 113 °C)for complex CA10B1N	102
Fig. 3-5.10 P _s value dependence on: (a) voltage variation at f = 60 Hz, T = 113 °C, (b) frequency variation at V _{pp} = 322, T = 113 °C.	104
Fig 3-5.11 Switching current curves observed for copolymer CA10B1N under a modified triangular wave field with a pause at 0 V: (a) at 113 °C,	

(b) respectively in the isotropic (244 °C), crystalline (72 °C), liquid
crystal state (114 °C)104

Fig. 3-5.12 (a) A profile showing the time dependence of the polarization
current obtained for the SmCP_F phase of complex **CA10C1N** under a
triangular wave field (V_{pp} = 411 V, f = 150 Hz). (b) P_s value was varied
with frequency at a fixed voltage, V_{pp} = 411 V.....105



表目錄

Table 1-1.1 The Classification of Liquid Crystalline.....	5
Table 2-4.1 Composition in Feed and Polymerization Conditions of Homo- and Copolymers.....	61
Table 3-2.1. Transition Temperatures and Corresponding Enthalpy Values (in brackets) of Investigated Compounds.....	67
Table 3-2.2 Comparison of Molecular Lengths (L), Lattice Parameters of the Col _r Phase (a,c), and Layer Spacing Value in the SmCP _A Phase (d).....	70
Table 3-3.1 Transition Temperatures and Corresponding Enthalpy Values (in brackets) of H-bonded Molecules.....	78
Table 3-4.1 Transition Temperatures and Corresponding Enthalpy Values (in brackets) of Acrylate Monomers.....	87
Table 3-5.1 Input and Output Constitutional Ratio and Thermal Properties of All Polymers.....	93
Table 3-5.2 Transition Temperatures and Corresponding Enthalpy Values (in brackets) of Homopolymers/Copolymers.....	98
Table 3-5.3 X-ray Data for Some Studied Materials.....	101